NLO QCD corrections to top quark pair production and decay at hadron colliders

JHEP08(2009)049

(http://iopscience.iop.org/1126-6708/2009/08/049)

Published by IOP Publishing for SISSA

Received: *July 22, 2009*
Accepted: *July 31, 2009*
Published: *August 12, 2009*

JHEP08(2009)049

NLO QCD corrections to top quark pair production and decay at hadron colliders

Kirill Melnikov and Markus Schulze

Department of Physics and Astronomy, Johns Hopkins University, Baltimore, MD 21218, U.S.A.

E-mail: melnikov@pha.jhu.edu, schulze@pha.jhu.edu

Abstract: We present results for the next-to-leading order QCD corrections to the production and semi-leptonic decays of a top quark pair in hadron collisions, retaining all spin correlations. To evaluate the virtual corrections, we employ generalized D-dimensional unitarity. The computation is implemented in a numerical program which allows detailed studies of $t\bar{t}$-related observables at the Tevatron and the LHC.

Keywords: QCD Phenomenology

ArXiv ePrint: 0907.3090

doi:10.1088/1126-6708/2009/08/049

Contents

JHEP08(2009)049

1 Introduction

The production of top quark pairs is an interesting process for understanding QCD dynamics. The very short life-time of a top quark and its large mass enable accurate theoretical predictions for this process for all energies, including close to $t\bar{t}$ threshold. One can then use the $t\bar{t}$ production to study properties of the top quark, such as the value of the top quark mass, branching fraction $\Gamma(t \to Wb)/\Gamma_{\rm tot}$ etc. In addition, the short life-time and large mass of the top quark have important consequences for top quark polarization since non-perturbative fluctuations of chromomagnetic field are too weak to change the direction of the top quark spin. Hence, in the absence of hard gluon radiation, top quark polarization is conserved; information about it can be obtained from properties of the top quark decay products. This information can be used to study the Lorentz structure of interaction vertices involved in top quark production and decay. Also, one can use top quark spin correlations to distinguish different production mechanisms, e.g. $q\bar{q} \to t\bar{t}$ from $gg \to t\bar{t}$, at least in certain kinematic limits. This rich physics is fully reflected in an experimental top quark program at the Tevatron, which is the primary source of our knowledge about top quark properties. The summary of recent experimental results can be found in refs. [1–3].

On the other hand, as was repeatedly emphasized in the past, top quark physics at the LHC is not just a rescaled version of the top quark physics at the Tevatron. Indeed, the high energy and luminosity of the LHC will lead to a dramatic increase in the number of observed $t\bar{t}$ events. As the result, interpretations of cross-section measurements will be subject to theoretical uncertainties rather than statistical errors. This fact motivated recent analysis [4–6] and reviews [2, 3, 7] where the quality of current understanding of $t\bar{t}$ production was thoroughly assessed.

We point out in this regard that pioneering studies of heavy quark production cross-sections at next-to-leading order (NLO) in QCD were performed almost twenty years ago [8,

9].[1] These computations were further extended to cover various kinematic distributions of the produced top quarks in refs. [11, 12]. In addition, threshold resummation was applied to top quark production at the Tevatron and the LHC [13], although its practical relevance for $t\bar{t}$ production at both colliders is still an issue of debate. Soft gluon corrections and Coulomb gluon bound state corrections were combined in ref. [14] to provide an accurate description of $t\bar{t}$ threshold region. Electroweak corrections to $\sigma_{t\bar{t}}$ were studied in ref. [15]. There is an ongoing effort to compute next-to-next-to-leading order QCD corrections to top quark pair production in hadron collisions [16].

In all studies of top production described so far top quarks were treated as stable particles and summation over their spin degrees of freedom was performed. This approach introduces two problems. First, spin degrees of freedom of top quarks influence kinematics of their decay products and in this way lead to observable consequences. Second, there are QCD radiative corrections related to the decay, rather than production, stages of the time evolution of $t\bar{t}$ system. Given the fact that the $t\bar{t}$ production cross-section at the LHC is very large, a degree of realism in its description is clearly warranted. To achieve it, we require a NLO QCD prediction for $t\bar{t}$ production that is valid at the level of observable particles, such as leptons, quarks and gluons originating *either* from production of top quarks or in their decays. In principle, this seems to necessitate a next-to-leading computation for $2 \to 4$ processes such as $pp \to \ell^+\nu\ell^-\bar{\nu}b\bar{b}$ or $pp \to u\bar{d}\ell^-\bar{\nu}b\bar{b}$, which is a formidable task at present.

Fortunately, the problem can be simplified by studying double resonance contributions, but accounting for spin degrees of freedom exactly through all stages of the top quark decay chain. Indeed, when top quarks are treated as truly unstable particles, all QCD corrections to a relevant $2 \to 4$ process[2] can be decomposed into factorizable and non-factorizable [17]. Non-factorizable corrections imply a cross-talk between production and decays of top quarks. In the limit $\Gamma_t/m_t \to 0$, these corrections must vanish since quantum interference should not occur if events are separated by macroscopic distances. The precise way in which such non-factorizable corrections vanish was described in refs. [17–19]. In what follows we work in the on-shell approximation for top quarks, ignoring non-factorizable corrections.

Once non-factorizable corrections are neglected, a full description of $t\bar{t}$ production and decay including all the spin correlations is achieved by computing NLO QCD corrections to both production and decay of a *polarized* $t\bar{t}$ pair. In an impressive series of papers [20–22] Bernreuther, Brandenburg, Si and Uwer computed the spin density matrix for the production of a $t\bar{t}$ pair in hadron collisions through NLO QCD. Corrections to decays of polarized top quarks were obtained in refs. [23, 24]. Putting all these bits together, Bernreuther et al. studied a number of kinematic distributions which can be used at hadron colliders to probe top quark spin correlations [25, 26].

While the importance of accurate predictions of top quark spin correlations was strongly emphasized in refs. [25, 26], to the best of our knowledge there is no publicly

[1] It is interesting to point out that *analytic* results for NLO QCD corrections to top production in $gg, q\bar{q}$ and qg channels were obtained very recently in ref. [10].

[2] We mean here the final state $W^+W^-b\bar{b}$.

JHEP08(2009)049

available numerical program that satisfies the following requirements:

- it containts NLO QCD corrections to top quark production and decay;
- it includes all spin correlations for the processes $pp \to \ell^+\nu\ell^-\bar{\nu}b\bar{b}$ and $pp \to u\bar{d}\ell^-\bar{\nu}b\bar{b}$;
- it allows arbitrary cuts on particles in the final state.

While the implementation of heavy flavor production in MC@NLO [27] and POWHEG [28] comes close to these requirements (see e.g. [29]), those programs do not fully include all spin correlations through NLO QCD. It seems to us that developing a numerical program with capabilities listed above is useful since it will contribute to more realistic description of $t\bar{t}$ production at hadron colliders. Computing NLO QCD corrections to $t\bar{t}$ production and decay and implementing them into a flexible numerical program is the primary goal of this paper.

Another motivation for undertaking the study of $t\bar{t}$ production is more theoretical — we would like to explore how unitarity-based methods for one-loop computations work in a relatively simple but fully realistic setting, when massive particles are involved. Initial studies of $t\bar{t}$ production in the context of generalized D-dimensional unitarity [30] were performed in ref. [31]. Those results were extended by us with an eye on applying generalized D-dimensional unitarity to $t\bar{t}$ production in association with jets.[3] The simplest application — the case of polarized $t\bar{t}$ production — is described in this paper.

The rest of the paper is organized as follows. In section 2 some theoretical aspects of the computation are discussed. In section 3 we present a number of observables relevant for $t\bar{t}$ studies at the Tevatron and the LHC. We conclude in section 4. More details on the calculation of virtual and real corrections are described in appendices A and B, respectively.

2 Theoretical framework

In this section the theoretical framework relevant for the computation is briefly described. As already pointed out in the Introduction, we study the production of top quarks and allow for their semileptonic decays. We include all the spin correlations but keep top quarks on their mass shells. We do not consider hadronic decays of top quarks in this paper.

We first discuss an efficient way to incorporate top quark decays into the computation.[4] The tree amplitude for the process $ij \to \bar{t}t \to (\bar{b}\ell^-\bar{\nu})(b\ell^+\nu)$ can be written as

$$A^{\text{tree}} = \left(\tilde{A}(t \to b\ell^+\nu) \, \frac{\mathrm{i}(\not{p}_t + m_t)}{p_t^2 - m_t^2 + \mathrm{i}m_t\Gamma_t} \right) \tilde{A}(ij \to \bar{t}t) \left(\frac{\mathrm{i}(-\not{p}_{\bar{t}} + m_t)}{p_{\bar{t}}^2 - m_t^2 + \mathrm{i}m_t\Gamma_t} \, \tilde{A}(\bar{t} \to \bar{b}\ell^-\bar{\nu}) \right), \tag{2.1}$$

where $\tilde{A}(ij \to \bar{t}t)$ and $\tilde{A}(\overset{(-)}{t} \to \overset{(-)}{b}\ell^{\pm}\overset{(-)}{\nu})$ are sub-amplitudes for production and decay processes, top quark propagators are factored out and summation over spinor indices is

[3] We point out that NLO QCD corrections to $t\bar{t}$ + jet production at the LHC and the Tevatron were reported in [32, 33].

[4] We are grateful to Keith Ellis for emphasizing this point to us.

implicit. Note that in eq. (2.1) the top quarks are off the mass-shell. To compute the cross-section, we need to square the amplitude A^{tree} and integrate it over the phase-space for final state particles. To simplify this procedure, we approximate the squared amplitude by taking the limit $\Gamma_t/m_t \to 0$. In this approximation, propagators that appear in eq. (2.1) yield

$$\left.\frac{1}{(p_t^2 - m_t^2)^2 + m_t^2\Gamma_t^2}\right|_{\Gamma_t/m_t\to 0} = \frac{2\pi}{2m_t\Gamma_t}\,\delta(p_t^2 - m_t^2). \tag{2.2}$$

After factorizing the phase-space integral into the phase-space for a $t\bar{t}$ pair and the decay phase-spaces for t and $\bar{t}$, the delta-function in eq. (2.2) forces top quarks on their mass-shells. This separates the production stage from the decay stage and allows us to implement top quark decays by choosing the on-shell spinors

$$\bar{U}(p_t) = \tilde{A}(t \to b\ell^+\nu)\,\frac{\mathrm{i}(\not{p}_t + m_t)}{\sqrt{2m_t\Gamma_t}}, \tag{2.3}$$

$$V(p_{\bar{t}}) = \frac{\mathrm{i}(-\not{p}_{\bar{t}} + m_t)}{\sqrt{2m_t\Gamma_t}}\,\tilde{A}(\bar{t} \to \bar{b}\ell^-\bar{\nu}), \tag{2.4}$$

to describe polarization states of top quarks. eq. (2.1) can now be rewritten as

$$A^{\text{tree}} = \bar{U}(p_t)\,\tilde{A}(ij \to \bar{t}t)\,V(p_{\bar{t}}) + \mathcal{O}\left(\frac{\Gamma_t}{m_t}\right). \tag{2.5}$$

The usefulness of eqs. (2.3)–(2.5) is twofold. First, since $\bar{U}$ and V are on-shell Dirac spinors, the amplitude A^{tree} can be computed in a conventional way; this means that the inclusion of t and $\bar{t}$ decays does not increase the complexity of scattering amplitudes that need to be calculated. Second, eq. (2.5) actually helps in *reducing* computational burden. Indeed, the top quark spinors depend on polarization states and momenta of leptons, neutrinos and b-quarks which we treat as massless. For top quark decays, helicity states of all massless particles are fixed, due to the $V-A$ structure of flavor-changing interaction vertices in the Standard Model. This implies that the spinors $\bar{U}$ and V have *uniquely defined polarizations* and no helicity sums related to t and $\bar{t}$ are involved in the cross-section computation. In the evaluation of the decay amplitudes we keep the W-boson on-shell and treat the b-quark as massless particle.

Having discussed how to deal with t and $\bar{t}$ decays efficiently, we focus on other computational details. The on-shell approximation for top quarks splits all the QCD effects into corrections to the production and corrections to the decay. These corrections do not interfere since production and decay stages are separated by large space-time intervals. As the result, $t\bar{t}$ production with NLO QCD effects and $t(\bar{t})$ decay with NLO QCD effects can be treated as independent processes.

We begin with corrections to $t\bar{t}$ production process. In this case, as we just discussed, all one has to do to incorporate top quark decays, is to use in eq. (2.5) the on-shell spinors for t and $\bar{t}$, shown in eqs. (2.3)–(2.4). This prescription is valid both at leading and at next-to-leading order. We organize the calculation in terms of gauge-invariant color ordered sub-amplitudes. Each such amplitude multiplies a specific color factor and has a fixed ordering

JHEP08(2009)049

of external particles. We use Berends-Giele [34] recurrence relations to evaluate those sub-amplitudes for each contributing helicity configuration at leading order. There are two partonic processes that need to be considered for LO, and virtual component of NLO computations – $gg \to t\bar{t}$ and $q\bar{q} \to t\bar{t}$. Their color decomposition is given in appendix A.

For the computation of virtual corrections to $t\bar{t}$ production, we employ the method of generalized D-dimensional unitarity [30]. The basic idea of this method is to consider unitarity cuts of scattering amplitudes in D-dimensional space-times where $D > 4$ is *integer*. It turns out that dimensionally-regularized one-loop amplitudes can be fully reconstructed from these unitarity cuts provided that *tree-level* on-shell scattering amplitudes for complex external momenta, evaluated in six- and eight-dimensional space-times, are available. As pointed out in ref. [35], the unitarity approach can be suitably implemented using the so-called OPP reduction technique [36]. For a detailed description of the method see ref. [30].

We turn to the discussion of real emission corrections to $t\bar{t}$ production. Real emission processes develop singularities when a massless final state particle is unresolved, i.e. it is soft and/or collinear to another particle. When integrated over the unresolved phase-space, those singularities produce divergencies that cancel against divergencies in virtual corrections and unrenormalized parton distribution functions, yielding finite cross-sections. In order to treat real emission singularities in a numerically stable way we employ an extension of Catani-Seymour dipole subtraction scheme [37] to massive particles [38]. Recall that the basic idea of the subtraction procedure is to construct an approximation to matrix elements squared of real emission processes that, on one hand, has the same singular limits as real emission matrix elements and, on the other hand, can be analytically integrated over the phase-space of unresolved particles. Because top quarks are heavy, they never appear as unresolved particles and their spin degrees of freedom are not essential for the construction of the subtraction terms. Hence, we can also use the $\bar{U}, V$ spinors to compute (subtracted) real emission corrections and in this way account for decays of top quarks exactly. The color decomposition of amplitudes needed for the real corrections to the $t\bar{t}$ production process is given in appendix A. Furthermore, a list of all dipole subtraction terms is given in appendix B.

We now turn to the discussion of NLO QCD corrections to the top quark decay. Corrections to decay rate and lepton kinematic distributions in decays of polarized top quarks are well-known [23, 39]. However, since we want to keep our computation completely differential, to allow for arbitrary cuts on the final state particles, we need to go beyond the computation of ref. [23]. A detailed discussion of how such a computation should be set up was given recently for the case of single top production in ref. [40] and we closely follow that reference in our implementation of virtual and real QCD corrections to top quark decays.

We also point out that we use $\Gamma_t^{\rm LO}$ and $\Gamma_t^{\rm NLO}$ to construct top quark spinors in eqs. (2.3)–(2.4) in LO and NLO computations, respectively. Indeed if no restrictions on final state particles are applied, the cross-section computed in the on-shell approximation is given by the product of the $t\bar{t}$ production cross-section multiplied by t and $\bar{t}$ decay branching fractions. Since this statement holds true to all orders in perturbation theory, the

JHEP08(2009)049

width in eqs. (2.3)–(2.4) should also be computed in series of α_s, for consistency. Hence, the complete NLO cross-section can schematically be written as

$$\begin{aligned} \mathrm{d}\sigma^{\mathrm{NLO}} = \mathrm{d}\sigma^0 \, \frac{\mathrm{d}\Gamma_{\bar{t}}^0 \, \mathrm{d}\Gamma_t^0}{(\Gamma^0)^2} \; + \; \mathrm{d}\sigma^1 \, \frac{\mathrm{d}\Gamma_{\bar{t}}^0 \, \mathrm{d}\Gamma_t^0}{(\Gamma^0)^2} \\ + \, \mathrm{d}\sigma^0 \left(\frac{\mathrm{d}\Gamma_{\bar{t}}^1 \, \mathrm{d}\Gamma_t^0}{(\Gamma^0)^2} + \frac{\mathrm{d}\Gamma_{\bar{t}}^0 \, \mathrm{d}\Gamma_t^1}{(\Gamma^0)^2} \right) \; - \; \mathrm{d}\sigma^0 \, \frac{2\Gamma_t^1}{\Gamma_t^0} \, \frac{\mathrm{d}\Gamma_{\bar{t}}^0 \, \mathrm{d}\Gamma_t^0}{(\Gamma^0)^2} \end{aligned} \tag{2.6}$$

where σ^0, Γ^0 and σ^1, Γ^1 denote leading and next-to-leading order contributions to the production and decay processes, respectively. The last term in eq. (2.6) arises from the correction to the top quark width in eqs. (2.3)–(2.4).

To conclude this section, we mention checks that we applied to our computation to ensure its correctness. Within the unitarity method, one computes scattering amplitudes for particular polarization states of external particles. As the result, gauge invariance of all one-loop amplitudes involving external gluons can be easily checked by substituting polarization vector of a gluon by its momentum. One can also check the threshold $s \to 4m_t^2$ behavior of one-loop amplitudes, relevant for $t\bar{t}$ production. Indeed, close to $t\bar{t}$ threshold, scattering amplitudes are dominated by the Coulomb singularity and we checked that our implementation of the virtual corrections reproduces the Coulomb singularity correctly. The cancellation of infra-red and collinear divergencies between virtual and real corrections was checked numerically. Furthermore, the implementation of both virtual and real corrections was checked by comparing results for physical observables produced by our code against other programs that compute the $t\bar{t}$ production cross-section without top decays. We have extensively used MadGraph [41] and MCFM [42] for these comparisons to check LO and NLO results, respectively. In order to ensure the correctness of our implementation of top quark decays we checked that the NLO QCD corrections reproduce known results for the top width if no restrictions on final state particles are applied. Finally, we have checked that our code reproduces NLO QCD corrections to some observables sensitive to top quark spin correlations, discussed in ref. [26].

3 Results

We have implemented NLO QCD corrections to the production and semileptonic decays of a top quark pair in a FORTRAN program. The goal of this section is to illustrate some of its potential applications. Before discussing those examples, we describe the input parameters that are used in all numerical results presented in this paper.

We consider production of $t\bar{t}$ pairs both at the Tevatron and the LHC. The Tevatron center of mass energy is $\sqrt{s} = 1.96$ TeV and the LHC center of mass energy is $\sqrt{s} = 10$ TeV. We use the pole mass of the top quark, $m_t = 172$ GeV. The strong coupling constant α_s is renormalized in the $\overline{\mathrm{MS}}$ scheme except for top quark loop contributions to gluon self-energy diagrams that are subtracted at zero gluon momentum. We employ CTEQ6L1 parton distribution functions for leading order and CTEQ6.1M for next-to-leading order computations [43, 44]; those PDF sets correspond to $\alpha_s(m_Z) = 0.130$ and $\alpha_s(m_Z) = 0.118$ respectively. The mass of the W is taken to be $m_W = 80.419$ GeV. W couplings to

JHEP08(2009)049

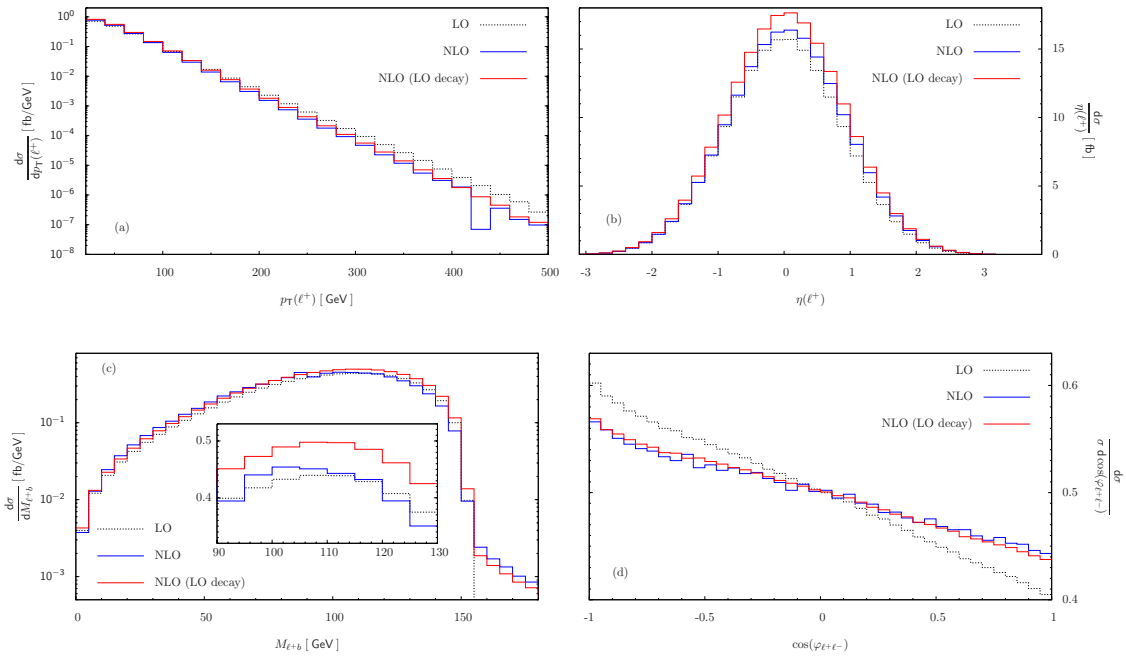

Figure 1. Various kinematic distributions for leptonic final states in $t\bar{t}$ production at the Tevatron. We show transverse momentum (a) and rapidity (b) distributions of the positively charged lepton as well as the distribution in the invariant mass of a lepton and a b-jet (c). The distribution in the (particularly defined, see text) opening angle of the leptons is shown in (d). Each distribution in panel (d) is normalized to the corresponding total cross-section. All cuts described at the beginning of section III are applied.

fermions are obtained from the Fermi constant $G_F = 1.16639 \cdot 10^{-5}\,\text{GeV}^{-2}$. The leading order width of the top quark is $\Gamma_t^{\text{LO}} = 1.47$ GeV and $\Gamma_t^{\text{NLO}} = 1.31$ GeV at next-to-leading order.[5] We use $|V_{tb}| = 1$ and employ on-shell approximation for the W boson, produced in $t \to Wb$ decays.

We set the width of the W boson to 2.14 GeV. We consider this to be an experimentally measured width of the W boson, not the result of computation in leading order of QCD perturbation theory. This implies that our leading order prediction for $pp \to t\bar{t} \to \ell^+\nu\ell^-\bar{\nu}b\bar{b}$ includes the NLO QCD branching ratio for $W \to e\nu$. While simple, this effect is definitely not negligible numerically — since $\mathcal{O}(\alpha_s)$ corrections increase the W width by approximately $2.5 - 3$ percent, the use of LO or NLO branching fractions for W bosons changes the cross-section for $pp \to t\bar{t} \to \ell^+\nu\ell^-\bar{\nu}b\bar{b}$ by five to six percent.

To define jets, we use the $k_\perp$-clustering algorithm [45] with $R = 0.4$. We require that two b-jets are present in the event. We define jet flavor through its "bottomness" quantum number so that, for example, a jet that contains b and $\bar{b}$ is not a b-jet. We point out that this definition is infra-red safe through NLO QCD approximation for $t\bar{t}$ production whereas this is not true in general, for massless quarks [46]. For b-jets we require a minimal

[5] This result for Γ_t^{NLO} is obtained by choosing the renormalization scale for the strong coupling constant to be the top quark mass.

JHEP08(2009)049

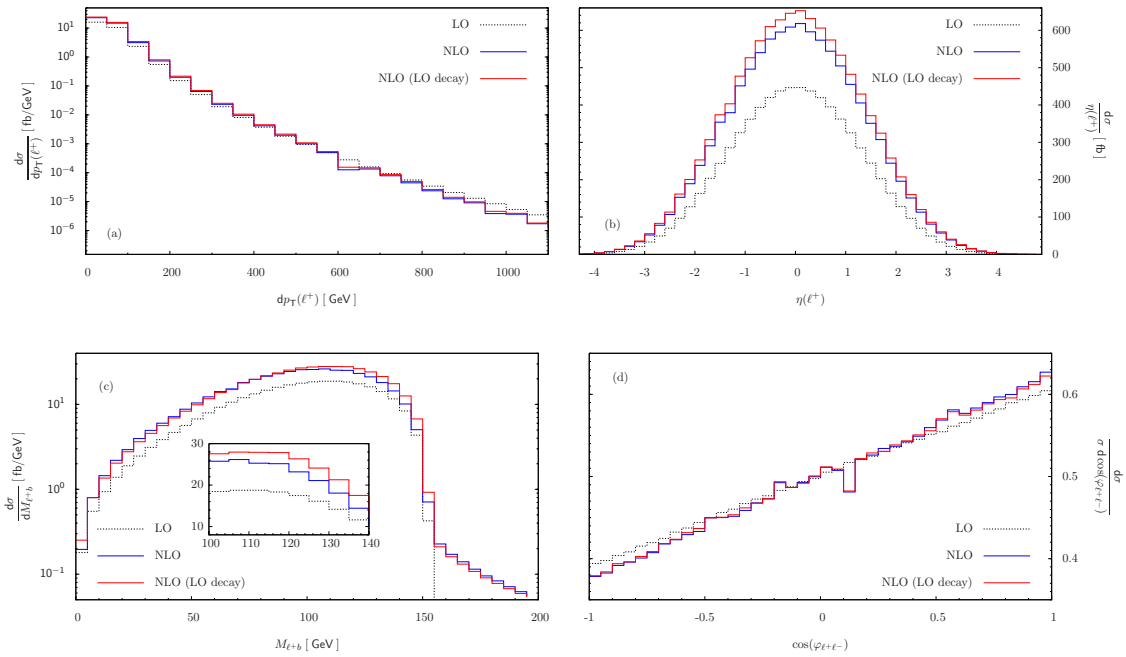

Figure 2. Various kinematic distributions for leptonic final states in $t\bar{t}$ production at the LHC. We show transverse momentum (a) and rapidity (b) distributions of the positively charged lepton as well as the distribution in the invariant mass of a lepton and a b-jet (c). The distribution in the (specially defined, see text) opening angle of the leptons is shown in (d). Each distribution in panel (d) is normalized to the corresponding total cross-section. All cuts described at the beginning of section III are applied.

transverse momentum of 20 GeV. Charged leptons must be produced with the transverse momentum larger than 20 GeV and the missing energy in the event should exceed 40 GeV. We also set renormalization and factorization scales to the value of the top quark mass. Since scale dependence of various observables for $t\bar{t}$ production was studied in detail in the existing literature, we do not present such studies in this paper.

To set the scale for the magnitude of next-to-leading QCD effects in $t\bar{t}$ production for our choices of input parameters, we quote results for cross-sections at leading and next-to-leading order for the Tevatron ($p\bar{p} \to t\bar{t} \to bl^+\nu\bar{b}l^-\bar{\nu}$)

$$\sigma_{\rm LO} = 34.63\,{\rm fb}, \quad \sigma_{\rm NLO} = 36.47\,{\rm fb}, \quad K_{\rm TEV} = \frac{\sigma_{\rm NLO}}{\sigma_{\rm LO}} = 1.05, \tag{3.1}$$

and the LHC ($pp \to t\bar{t} \to bl^+\nu\bar{b}l^-\bar{\nu}$)

$$\sigma_{\rm LO} = 1484\,{\rm fb}, \quad \sigma_{\rm NLO} = 2097\,{\rm fb}, \quad K_{\rm LHC} = \frac{\sigma_{\rm NLO}}{\sigma_{\rm LO}} = 1.41. \tag{3.2}$$

To obtain those numbers, we set the renormalization and factorization scales to m_t and apply all the cuts listed in the beginning of this section.

We are now in position to illustrate capabilities of our numerical program by presenting a number of $t\bar{t}$-related kinematic distributions, computed through NLO in perturbative

JHEP08(2009)049

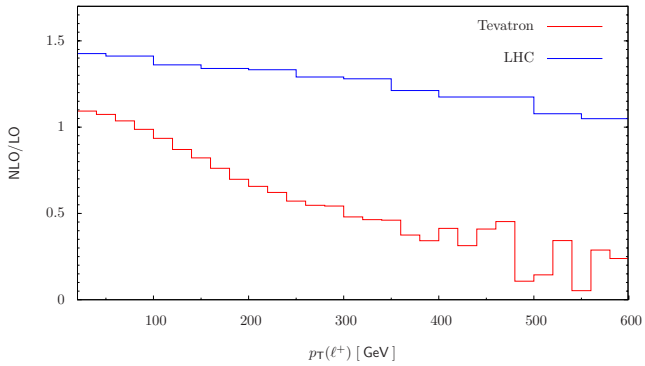

Figure 3. The ratio of NLO to LO predictions for ℓ^+ transverse momentum distributions, for the Tevatron and the LHC. The input parameters are described at the beginning of section III.

QCD. In figure 1 we present results for the Tevatron. The transverse momentum and rapidity distributions of leptons in top decays are shown in figures 1(a) and 1(b), respectively. The distribution in the invariant mass of the charged lepton and the b-jet is given in figure 1(c). Figure 1(d) shows the distribution in $\cos\varphi_{\ell^+\ell^-}$, where $\varphi_{\ell^+\ell^-}$ is the angle between the directions of flight of ℓ^+ and ℓ^-, defined in the rest frames of t and $\bar{t}$ respectively. In all cases we compare predictions at leading and next-to-leading order, with and without corrections to the decay. Corresponding results for the LHC are shown in figure 2.

We first consider transverse momentum and rapidity distributions of the charged lepton, shown in the upper panels of figures 1, 2. Both of these distributions are standard but effects of QCD corrections to top decays and top spin correlations are never included in their computation. For both of these observables NLO QCD effects are important. For example, as we show in figure 3, the shape of the transverse momentum distribution changes significantly at the Tevatron while at the LHC similar change is smaller, but non-negligible. For the charged lepton rapidity distribution, NLO QCD corrections to decays are important, especially at central rapidities at the Tevatron.

Another distribution that we show in figures 1, 2 is the distribution in the invariant mass of a positively charged lepton ℓ^+ and a b-jet, M_{ℓ^+b}. This observable is interesting for a number of reasons. First, a (kinematically) similar observable — an invariant mass of ℓ^+ and J/ψ originating from B meson decay – was discussed in connection with the measurement of the top quark mass in ref. [47]. Similar to J/ψ ℓ^+ invariant mass, the invariant mass of the b-jet and ℓ^+ has a clear kinematic boundary at leading order, see figures 1, 2. This boundary $\max(M^2_{\ell^+b}) = m_t^2 - m_W^2$ is the consequence of the on-shell conditions for the top quark and the W boson. Those conditions lead to a lower bound on the allowed neutrino energy in the top quark rest frame E_ν and to the upper bound on $M^2_{\ell^+b} = m_t^2 - 2m_t E_\nu$. The existence of the kinematic boundary makes this observable potentially interesting for the top quark mass determination. In addition, M_{ℓ^+b} belongs to a general class of observables that may be used to study spins of Beyond the Standard Model particles at the LHC. The effect of NLO QCD corrections on the M_{ℓ^+b} distribution is interesting. For example, at the Tevatron there is a significant cancellation between

JHEP08(2009)049

corrections to $t\bar{t}$ production and corrections to t and $\bar{t}$ decays for this observable. This effect also exists at the LHC although it is less pronounced.

It is interesting that once the NLO QCD corrections are included, events start to appear beyond the leading order kinematic boundary and both, QCD corrections to the production and QCD corrections to the decay contribute. The origin of these events is peculiar since they appear as the consequence of the fact that the momentum of the b-jet rather than the momentum of the b-quark is employed in the calculation of M_{ℓ^+b}. Then, for example, a gluon emitted in the decay of $\bar{t}$ may combine with the b-quark from top decay to form a b-jet. The energy of such a jet is not restricted by on-shell conditions applied to t and W. As the result, the invariant mass of the b-jet and ℓ^+ may exceed the LO kinematic boundary. A similar mechanism is in effect when gluon emission occurs as part of the top production process. Note, however, that if a gluon is emitted in the decay of a *top* quark $t \to b\ell^+\nu + g$, then the invariant mass of a b-jet and ℓ^+ can not exceed the leading-order kinematic boundary.

Finally, we discuss lepton angular correlations; such observables are particularly sensitive to correct implementation of spin correlations in $t\bar{t}$ production and decay. Indeed, angular correlations tell us whether leptons prefer to be produced with parallel or anti-parallel momenta and, as it turns out, the answer to this question differs for the Tevatron and the LHC [7]. To understand the difference recall the two mechanisms that dominate the $t\bar{t}$ pair production at those colliders. At the Tevatron, top pairs are mostly produced in an annihilation of a $q\bar{q}$ pair — $q\bar{q} \to g^* \to t\bar{t}$ – which forces a $t\bar{t}$ pair to have angular momentum $J = 1$. Since, in addition, most of the time the annihilation occurs close to $t\bar{t}$ threshold, it is most probable that the $t\bar{t}$ pair is produced in an S-wave with spins of t and $\bar{t}$ parallel, to create a $J = 1$ state. Since e^+ likes to follow the direction of t spin while e^- prefers the direction opposite to $\bar{t}$ spin, flight directions of e^+ and e^- are anti-correlated.

At the LHC the situation is different since $gg \to t\bar{t}$ annihilation becomes the dominant production channel. Close to $t\bar{t}$ threshold the largest contribution comes from an S-wave $J = 0$ color-octet annihilation [14]. This suggests that e^+ and e^- prefer to be produced with parallel momenta at the LHC, at least to an extent that threshold production is important there.

In figures 1(d), 2(d) we show the opening angle distribution between two charged leptons at the LHC and the Tevatron. Note that the flight directions of ℓ^+ and ℓ^- are defined, respectively, in t and $\bar{t}$ *rest* frames, when computing this observable. Azimuthal correlations are substantial at LO and remain fairly pronounced even after NLO QCD corrections are included. It is interesting that NLO QCD effects are more important at the Tevatron where the shape of the distribution changes. At the LHC the NLO QCD effects do not change the shape of the distribution at all, so leading order predictions do a good job in that case. QCD corrections to top decays do not play an important role for this observable for both, the Tevatron and the LHC. We note that a similar distribution was computed through NLO QCD in refs. [25, 26], but no jet cuts were applied. However, by removing all the cuts in our computation and by adjusting the input parameters, we reproduce results for this distribution reported in refs. [25, 26].

One of the drawbacks of using $\cos\varphi_{\ell^+\ell^-}$ to study spin correlations is the requirement that t and $\bar{t}$ rest frames are reconstructed and, for semileptonic top decays, it is not possible

JHEP08(2009)049

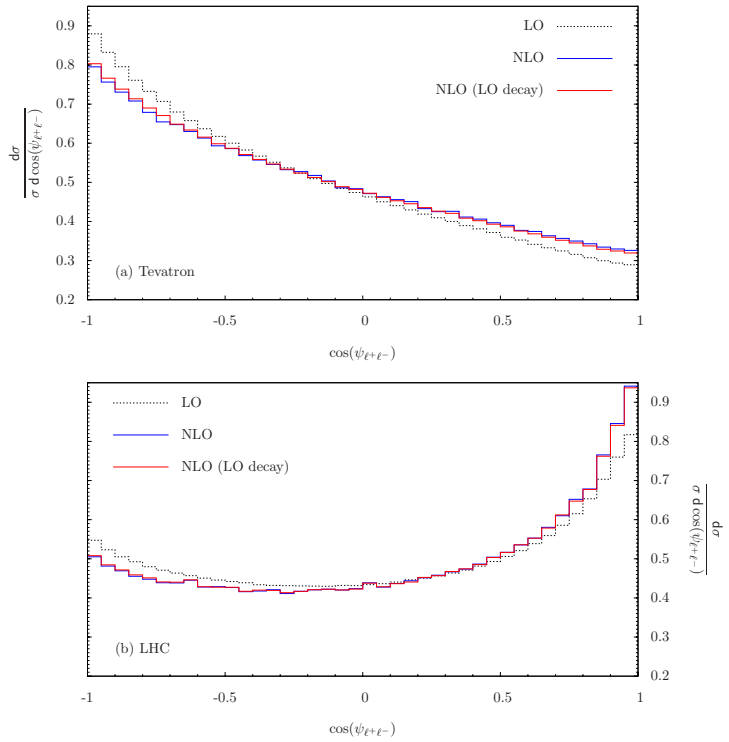

Figure 4. The distribution in the opening angle of the two leptons in the *laboratory frame*, normalized to the corresponding total cross-section. All cuts described at the beginning of section III are applied.

to do this unambiguously. In this respect, we would like to point out that $t\bar{t}$ spin correlations can also be studied using a much simpler observable — the opening angle $\psi_{\ell^+\ell^-}$ of the two leptons in the *laboratory frame*.[6] The corresponding distributions computed at leading and next-to-leading order are shown in figure 4 for both the Tevatron and the LHC. The results are similar to distributions in $\varphi_{\ell^+\ell^-}$ shown in figures 1(d), 2(d) but the effect of the radiative corrections on the shape of $\psi_{\ell^+\ell^-}$ distribution at the LHC is stronger.

To conclude this section, we point out that results reported here are not supposed to provide exhaustive phenomenological studies of $t\bar{t}$ production; rather, they should illustrate capabilities of our numerical implementation of NLO QCD corrections to $t\bar{t}$ production and decays. We have chosen to present a number of distributions which we find interesting but, as with any NLO QCD computation, essentially any infra-red safe observable can be calculated and analyzed. In this regard, a numerical program that allows to impose arbitrary cuts and employ arbitrary jet algorithms, includes all the spin correlations in $t\bar{t}$ production and in t and $\bar{t}$ decays and incorporates NLO QCD corrections to (semileptonic) decays of top quarks, is very attractive since it can be used for realistic description of $t\bar{t}$ pair production in hadron collisions.

[6] A similar observable was suggested in ref. [48].

JHEP08(2009)049

4 Conclusions

In this paper the computation of next-to-leading order QCD corrections to the production and decay of top quark pairs at the Tevatron and the LHC is presented. Our goal was to develop a numerical program which employes the on-shell approximation for top quarks, yet accounts for all the spin correlations in their production and semileptonic decays through NLO QCD.

To this end, the implementation of next-to-leading order corrections to the production and decay of polarized top quarks is required. We performed such an implementation at a fully differential level. This allows us to compute an arbitrary observable defined in terms of lepton momenta, missing energy and jet energies and momenta, originating either in top production or decay. We have illustrated the capabilities of the program by presenting a variety of differential distributions that are sensitive to top spin correlations and NLO QCD corrections to top quark decays.

An interesting aspect of the computation reported in this paper is that the method of generalized D-dimensional unitarity [30] is employed to compute virtual corrections to $t\bar{t}$ production cross-section; this is the first application of generalized D-dimensional unitarity to a fully realistic NLO computation that involves massive external and internal particles. We find that, in general, the method works well so its application to other processes with massive particles is definitely warranted.

Acknowledgments

We are grateful to Keith Ellis for useful conversations. This research is supported by the startup package provided by Johns Hopkins University.

A Color decomposition

In this appendix we summarize various results for the color decomposition of tree- and one-loop amplitudes that we used in this paper.

We begin with the leading order process. At leading order two partonic processes contribute to $t\bar{t}$ production: $gg \to t\bar{t}$ and $\bar{q}q \to t\bar{t}$. Their color decomposition is given by

$$A^{\rm tree}(gg \to t\bar{t}) = g_{\rm s}^2 \sum_{\sigma\in S_2} (T^{a_{\sigma_3}} T^{a_{\sigma_4}})_{i_2}^{\bar{i}_1}\, \mathcal{A}^{\rm tree}(1_{\bar{t}}, 2_t, (\sigma_3)_g, (\sigma_4)_g), \tag{A.1}$$

$$A^{\rm tree}(\bar{q}q \to t\bar{t}) = g_{\rm s}^2 \left[\delta_{i_4}^{\bar{i}_1}\delta_{i_2}^{\bar{i}_3} - \frac{1}{N_{\rm c}}\delta_{i_2}^{\bar{i}_1}\delta_{i_4}^{\bar{i}_3}\right] \mathcal{A}^{\rm tree}(1_{\bar{t}}, 2_t, 3_{\bar{q}}, 4_q) \tag{A.2}$$

where $\mathcal{A}^{\rm tree}(1_{\bar{t}}, 2_t, i, j)$ are color-ordered tree amplitudes and $g_{\rm s}$ is the strong coupling constant. The generators T^a of the $\mathrm{SU}(N_{\rm c}=3)$ color group are normalized to $\mathrm{Tr}(T^a T^b) = \delta^{ab}$ and satisfy the commutation relation $[T^a, T^b] = -F^c_{ab} T^c$.

Considering real emission contribution to top quark pair production at next-to-leading order, we find that four partonic processes contribute $gg \to \bar{t}tg$, $\bar{q}q \to \bar{t}tg$, $qg \to \bar{t}tq$, $\bar{q}g \to$

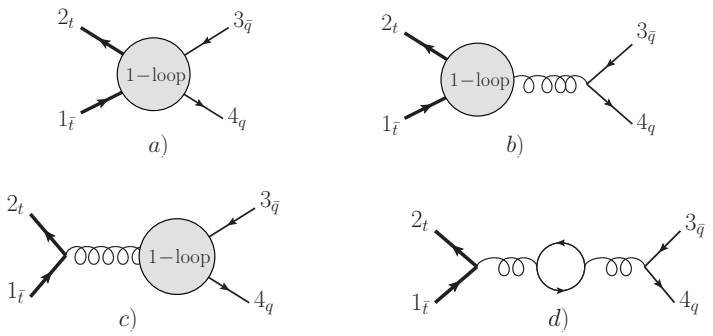

Figure 5. Definition of primitive amplitudes with four quarks. Figure a) defines $\mathcal{A}^a$ which includes all topologies where both external fermion lines enter the loop; figures b) and c) define $\mathcal{A}^b$ and $\mathcal{A}^c$ where either the top quark or the light quark line enter the loop, respectively; figure d) $\mathcal{A}^d$ includes topologies with a closed fermion loop.

$\bar{t}t\bar{q}$. The last three processes are related by crossing symmetry. The color decomposition for the two master processes is given by

$$A^{\text{tree}}(gg \to t\bar{t}g) = g_s^3 \sum_{\sigma\in S_3} (T^{a_{\sigma_3}} T^{a_{\sigma_4}} T^{a_{\sigma_5}})_{i_2}^{\bar{i}_1} \, \mathcal{A}^{\text{tree}}(1_{\bar{t}}, 2_t, (\sigma_3)_g, (\sigma_4)_g, (\sigma_5)_g), \quad \text{(A.3)}$$

$$\begin{aligned} A^{\text{tree}}(\bar{q}q \to t\bar{t}g) = g_s^3 \Big[& (T^{a_5})_{i_4}^{\bar{i}_1} \, \delta_{i_2}^{\bar{i}_3} \, \mathcal{A}^{\text{tree}}(1_{\bar{t}}, 2_t, 3_{\bar{q}}, 4_q, 5_g) \\ & + (T^{a_5})_{i_2}^{\bar{i}_3} \, \delta_{i_4}^{\bar{i}_1} \, \mathcal{A}^{\text{tree}}(1_{\bar{t}}, 2_t, 5_g, 3_{\bar{q}}, 4_q) \\ & + \frac{1}{N_c} (T^{a_5})_{i_2}^{\bar{i}_1} \, \delta_{i_4}^{\bar{i}_3} \, \mathcal{A}^{\text{tree}}(1_{\bar{t}}, 5_g, 2_t, 3_{\bar{q}}, 4_q) \\ & + \frac{1}{N_c} (T^{a_5})_{i_4}^{\bar{i}_3} \, \delta_{i_2}^{\bar{i}_1} \, \mathcal{A}^{\text{tree}}(1_{\bar{t}}, 2_t, 3_{\bar{q}}, 5_g, 4_q) \Big]. \end{aligned} \quad \text{(A.4)}$$

In the case of virtual amplitudes, a decomposition into color-ordered amplitudes is insufficient; instead, one has to consider the so-called primitive amplitudes [49]. We need one-loop amplitudes for $gg \to t\bar{t}$ and $q\bar{q} \to t\bar{t}$. For $gg \to t\bar{t}$ the color decomposition reads

$$\begin{aligned} A^{\text{virt}}(gg \to t\bar{t}) = g_s^4 \sum_{\sigma\in S_2} \Big[& (T^{x_2} T^{x_1})_{i_2}^{\bar{i}_1} (F^{a_{\sigma_4}} F^{a_{\sigma_3}})_{x_1 x_2} \, \mathcal{A}^{\text{L},[1]}(1_{\bar{t}}, 2_t, (\sigma_3)_g, (\sigma_4)_g) \\ & + (T^{x_2} T^{\sigma_3} T^{x_1})_{i_2}^{\bar{i}_1} (F^{a_{\sigma_4}})_{x_1 x_2} \, \mathcal{A}^{\text{L},[1]}(1_{\bar{t}}, (\sigma_3)_g, 2_t, (\sigma_4)_g) \\ & + (T^{x_1} T^{\sigma_4} T^{\sigma_3} T^{x_1})_{i_2}^{\bar{i}_1} \, \mathcal{A}^{\text{L},[1]}(1_{\bar{t}}, (\sigma_3)_g, (\sigma_4)_g), 2_t) \\ & + \sum_{f=1}^{N_f} (T^{a_{\sigma_3}} T^{a_{\sigma_4}})_{i_2}^{\bar{i}_1} \, \mathcal{A}_f^{\text{L},[1/2]}(1_{\bar{t}}, 2_t, (\sigma_3)_g, (\sigma_4)_g) \Big] \end{aligned} \quad \text{(A.5)}$$

where $\mathcal{A}^{\text{L},[s]}$ are left-primitive amplitudes, defined in ref. [49]. N_f is the number of quark flavors; top quarks in closed fermion loops are treated as massive particles.

For the virtual corrections to the process $\bar{q}q \to \bar{t}t$ we use the color decomposition

$$A^{\text{virt}}(\bar{q}q \to t\bar{t}) = g_s^4 \Big[\delta_{i_4}^{\bar{i}_1} \delta_{i_2}^{\bar{i}_3} \mathcal{B}_1 - \frac{1}{N_c} \delta_{i_2}^{\bar{i}_1} \delta_{i_4}^{\bar{i}_3} \mathcal{B}_2 \Big]. \quad \text{(A.6)}$$

JHEP08(2009)049

As the second term in eq. (A.6) vanishes after interference with the leading order amplitude we do not consider it here. The first term in eq. (A.6) is given by

$$\begin{aligned}\mathcal{B}_1 = &\left(N_c - \frac{2}{N_c}\right)\mathcal{A}^a(1_{\bar{t}}, 2_t, 3_{\bar{q}}, 4_q) - \frac{2}{N_c}\mathcal{A}^a(1_{\bar{t}}, 2_t, 4_q, 3_{\bar{q}}) \\ &+\frac{1}{N_c}\Big(\mathcal{A}^b(1_{\bar{t}}, 2_t, 3_{\bar{q}}, 4_q) + \mathcal{A}^c(1_{\bar{t}}, 2_t, 3_{\bar{q}}, 4_q)\Big) - \sum_{f=1}^{N_f}\mathcal{A}_f^d(1_{\bar{t}}, 2_t, 3_{\bar{q}}, 4_q). \qquad \text{(A.7)}\end{aligned}$$

The ordered primitive amplitudes $\mathcal{A}^{a,b,c,d}$ correspond to different topologies depending on which fermion lines enter the loop, cf. figure 5.

B Dipole subtraction terms

Following the notation of ref. [37], the generic form of the subtraction terms for the partonic channels $g(1)\,g(2) \to \bar{t}(3)\,t(4)\,g(5)$ is given by twelve dipoles

$$\mathcal{D}_3^{15},\ \mathcal{D}_4^{15},\ \mathcal{D}_3^{25},\ \mathcal{D}_4^{25},\ \mathcal{D}^{15,2},\ \mathcal{D}^{25,1},\ \mathcal{D}_{35}^{1},\ \mathcal{D}_{35}^{2},\ \mathcal{D}_{45}^{1},\ \mathcal{D}_{45}^{2},\ \mathcal{D}_{35,4},\ \mathcal{D}_{45,3}. \qquad \text{(B.1)}$$

It is easy to see that identical list of dipoles is required to construct the subtraction terms for $\bar{q}(1)\,q(2) \to \bar{t}(3)\,t(4)\,g(5)$ partonic channel. Note, however, that the above dipoles differ for different partonic channels since they contain particular splitting kernels and reduced tree amplitudes. The processes $\overset{(-)}{q}(1)\,g(2) \to \bar{t}(3)\,t(4)\,\overset{(-)}{q}(5)$ develop only collinear singularities making a summation over all spectator particles unnecessary. We therefore choose

$$\tilde{\mathcal{D}}^{15,2},\ \tilde{\mathcal{D}}^{25,1} \qquad \text{(B.2)}$$

as subtraction terms which differ from the original dipoles eq. (B.1) only by their color factor. In fact, since collinear singularities are local in color space, no color correlations are required for the dipoles in eq. (B.2); the corresponding color factors are given by C_F and T_R for each dipole in eq. (B.2), respectively.

The auxiliary contribution from the dipole subtraction terms needs to be added back. We choose to implement those terms by separately integrating each dipole over the unresolved phase-space. Singularities of integrated dipoles cancel against singularities of virtual corrections and unrenormalized parton distribution functions, yielding finite result for the cross-section. For the implementation of both unintegrated and integrated dipoles we used results in refs. [38, 40]. Following refs. [40, 50, 51] we introduce a parameter α for all initial-state emitter dipoles which allows to cut off the dipole phase-space in non-singular regions. This helps to improve numerical stability of our code and provides a non-trivial check of the implementation of subtraction terms.

.

References

[1] CDF collaboration, V. Shary, *Top quark pair production cross section at Tevatron*, in the proceedings of the *Moriond 2009 QCD session*, March 7–14, La Thuile, Italy (2009) arXiv:0905.4464 [SPIRES].

JHEP08(2009)049

[2] W. Wagner, *Top quark physics in hadron collisions*, *Rept. Prog. Phys.* **68** (2005) 2409 [hep-ph/0507207] [SPIRES].

[3] R. Kehoe, M. Narain and A. Kumar, *Review of top quark physics results*, *Int. J. Mod. Phys.* **A 23** (2008) 353 [arXiv:0712.2733] [SPIRES].

[4] S. Moch and P. Uwer, *Theoretical status and prospects for top-quark pair production at hadron colliders*, *Phys. Rev.* **D 78** (2008) 034003 [arXiv:0804.1476] [SPIRES].

[5] M. Cacciari, S. Frixione, M.L. Mangano, P. Nason and G. Ridolfi, *Updated predictions for the total production cross sections of top and of heavier quark pairs at the Tevatron and at the LHC*, *JHEP* **09** (2008) 127 [arXiv:0804.2800] [SPIRES].

[6] N. Kidonakis and R. Vogt, *The Theoretical top quark cross section at the Tevatron and the LHC*, *Phys. Rev.* **D 78** (2008) 074005 [arXiv:0805.3844] [SPIRES].

[7] W. Bernreuther, *Top quark physics at the LHC*, *J. Phys.* **G 35** (2008) 083001 [arXiv:0805.1333] [SPIRES].

[8] P. Nason, S. Dawson and R.K. Ellis, *The one particle inclusive differential cross-section for heavy quark production in hadronic collisions*, *Nucl. Phys.* **B 327** (1989) 49 [*Erratum ibid.* **B 335** (1990) 260] [SPIRES].

[9] W. Beenakker, W.L. van Neerven, R. Meng, G.A. Schuler and J. Smith, *QCD corrections to heavy quark production in hadron hadron collisions*, *Nucl. Phys.* **B 351** (1991) 507 [SPIRES].

[10] M. Czakon and A. Mitov, *Inclusive heavy flavor hadroproduction in NLO QCD: the exact analytic result*, arXiv:0811.4119 [SPIRES].

[11] M.L. Mangano, P. Nason and G. Ridolfi, *Heavy quark correlations in hadron collisions at next-to- leading order*, *Nucl. Phys.* **B 373** (1992) 295 [SPIRES].

[12] S. Frixione, M.L. Mangano, P. Nason and G. Ridolfi, *Top quark distributions in hadronic collisions*, *Phys. Lett.* **B 351** (1995) 555 [hep-ph/9503213] [SPIRES].

[13] N. Kidonakis and G. Sterman, *Resummation for QCD hard scattering*, *Nucl. Phys.* **B 505** (1997) 321 [hep-ph/9705234] [SPIRES];
R. Bonciani, S. Catani, M.L. Mangano and P. Nason, *NLL resummation of the heavy-quark hadroproduction cross- section*, *Nucl. Phys.* **B 529** (1998) 424 [hep-ph/9801375] [SPIRES];
N. Kidonakis, E. Laenen, S. Moch and R. Vogt, *Sudakov resummation and finite order expansions of heavy quark hadroproduction cross sections*, *Phys. Rev.* **D 64** (2001) 114001 [hep-ph/0105041] [SPIRES];
N. Kidonakis and R. Vogt, *Next-to-next-to-leading order soft gluon corrections in top quark hadroproduction*, *Phys. Rev.* **D 68** (2003) 114014 [hep-ph/0308222] [SPIRES];
A. Banfi and E. Laenen, *Joint resummation for heavy quark production*, *Phys. Rev.* **D 71** (2005) 034003 [hep-ph/0411241] [SPIRES];
M. Czakon and A. Mitov, *On the soft-gluon resummation in top quark pair production at hadron colliders*, arXiv:0812.0353 [SPIRES].

[14] Y. Kiyo, J.H. Kühn, S. Moch, M. Steinhauser and P. Uwer, *Top-quark pair production near threshold at LHC*, *Eur. Phys. J.* **C 60** (2009) 375 [arXiv:0812.0919] [SPIRES].

[15] W. Beenakker et al., *Electroweak one loop contributions to top pair production in hadron colliders*, *Nucl. Phys.* **B 411** (1994) 343 [SPIRES];
C. Kao, G.A. Ladinsky and C.P. Yuan, *Leading weak corrections to the production of heavy top quarks at hadron colliders*, *Int. J. Mod. Phys.* **A 12** (1997) 1341 [SPIRES];

JHEP08(2009)049

W. Bernreuther, M. Fuecker and Z.G. Si, *Mixed QCD and weak corrections to top quark pair production at hadron colliders*, *Phys. Lett.* **B 633** (2006) 54 [hep-ph/0508091] [SPIRES];
J.H. Kühn, A. Scharf and P. Uwer, *Electroweak corrections to top-quark pair production in quark-antiquark annihilation*, *Eur. Phys. J.* **C 45** (2006) 139 [hep-ph/0508092] [SPIRES];
S. Moretti, M.R. Nolten and D.A. Ross, *Weak corrections to gluon-induced top-antitop hadro-production*, *Phys. Lett.* **B 639** (2006) 513 [*Erratum ibid.* **B 660** (2008) 607] [hep-ph/0603083] [SPIRES]; *Weak corrections to four-parton processes*, *Nucl. Phys.* **B 759** (2006) 50 [hep-ph/0606201] [SPIRES];
J.H. Kühn, A. Scharf and P. Uwer, *Electroweak effects in top-quark pair production at hadron colliders*, *Eur. Phys. J.* **C 51** (2007) 37 [hep-ph/0610335] [SPIRES];
W. Hollik and M. Kollar, *NLO QED contributions to top-pair production at hadron collider*, *Phys. Rev.* **D 77** (2008) 014008 [arXiv:0708.1697] [SPIRES];
W. Bernreuther, M. Fucker and Z.-G. Si, *Electroweak corrections to $t\bar{t}$ production at hadron colliders*, *Nuovo Cim.* **123B** (2008) 1036 [arXiv:0808.1142] [SPIRES].

[16] U. Langenfeld, S. Moch and P. Uwer, *New results for $t\bar{t}$ production at hadron colliders*, arXiv:0907.2527 [SPIRES];
M. Czakon, *Tops from light quarks: full mass dependence at two-loops in QCD*, *Phys. Lett.* **B 664** (2008) 307 [arXiv:0803.1400] [SPIRES];
R. Bonciani, A. Ferroglia, T. Gehrmann, D. Maître and C. Studerus, *Two-loop fermionic corrections to heavy-quark pair production: the quark-antiquark channel*, *JHEP* **07** (2008) 129 [arXiv:0806.2301] [SPIRES];
M. Czakon, A. Mitov and S. Moch, *Heavy-quark production in massless quark scattering at two loops in QCD*, *Phys. Lett.* **B 651** (2007) 147 [arXiv:0705.1975] [SPIRES]; *Heavy-quark production in gluon fusion at two loops in QCD*, *Nucl. Phys.* **B 798** (2008) 210 [arXiv:0707.4139] [SPIRES];
J.G. Korner, Z. Merebashvili and M. Rogal, *NNLO $O(\alpha_s^4)$ results for heavy quark pair production in quark-antiquark collisions: the One-loop squared contributions*, *Phys. Rev.* **D 77** (2008) 094011 [arXiv:0802.0106] [SPIRES];
B. Kniehl, Z. Merebashvili, J.G. Korner and M. Rogal, *Heavy quark pair production in gluon fusion at next-to- next-to-leading $O(\alpha_s^4)$ order: one-loop squared contributions*, *Phys. Rev.* **D 78** (2008) 094013 [arXiv:0809.3980] [SPIRES];
C. Anastasiou and S.M. Aybat, *The one-loop gluon amplitude for heavy-quark production at NNLO*, *Phys. Rev.* **D 78** (2008) 114006 [arXiv:0809.1355] [SPIRES].

[17] V.S. Fadin, V.A. Khoze and A.D. Martin, *Interference radiative phenomena in the production of heavy unstable particles*, *Phys. Rev.* **D 49** (1994) 2247 [SPIRES];
K. Melnikov and O.I. Yakovlev, *Top near threshold: all α_S corrections are trivial*, *Phys. Lett.* **B 324** (1994) 217 [hep-ph/9302311] [SPIRES]; *Final state interaction in the production of heavy unstable particles*, *Nucl. Phys.* **B 471** (1996) 90 [hep-ph/9501358] [SPIRES].

[18] W. Beenakker, F.A. Berends and A.P. Chapovsky, *One-loop QCD interconnection effects in pair production of top quarks*, *Phys. Lett.* **B 454** (1999) 129 [hep-ph/9902304] [SPIRES].

[19] A. Denner, S. Dittmaier and M. Roth, *Non-factorizable photonic corrections to $e^+e^- \to WW \to 4$ fermions*, *Nucl. Phys.* **B 519** (1998) 39 [hep-ph/9710521] [SPIRES].

[20] W. Bernreuther, A. Brandenburg, Z.G. Si and P. Uwer, *Next-to-leading order QCD corrections to top quark spin correlations at hadron colliders: the reactions $gg \to t\bar{t}(g)$ and $gq(\bar{q}) \to t\bar{t}q(\bar{q})$*, *Phys. Lett.* **B 509** (2001) 53 [hep-ph/0104096] [SPIRES].

JHEP08(2009)049

[21] W. Bernreuther, A. Brandenburg, Z.G. Si and P. Uwer, *Top quark spin correlations at hadron colliders: predictions at next-to-leading order QCD*, *Phys. Rev. Lett.* **87** (2001) 242002 [hep-ph/0107086] [SPIRES].

[22] W. Bernreuther, A. Brandenburg, Z.G. Si and P. Uwer, *Top quark pair production and decay including spin effects at hadron colliders: predictions at NLO QCD*, *Int. J. Mod. Phys.* **A 18** (2003) 1357 [hep-ph/0111346] [SPIRES].

[23] A. Czarnecki, M. Jezabek and J.H. Kühn, *Lepton spectra from decays of polarized top quarks*, *Nucl. Phys.* **B 351** (1991) 70 [SPIRES].

[24] A. Brandenburg, Z.G. Si and P. Uwer, *QCD-corrected spin analysing power of jets in decays of polarized top quarks*, *Phys. Lett.* **B 539** (2002) 235 [hep-ph/0205023] [SPIRES].

[25] W. Bernreuther, A. Brandenburg, Z.G. Si and P. Uwer, *Top quark pair production and decay at hadron colliders*, *Nucl. Phys.* **B 690** (2004) 81 [hep-ph/0403035] [SPIRES].

[26] W. Bernreuther, A. Brandenburg, Z.G. Si and P. Uwer, *Investigation of top quark spin correlations at hadron collider*, hep-ph/0410197 [SPIRES].

[27] S. Frixione and B.R. Webber, *Matching NLO QCD computations and parton shower simulations*, *JHEP* **06** (2002) 029 [hep-ph/0204244] [SPIRES];
S. Frixione, P. Nason and B.R. Webber, *Matching NLO QCD and parton showers in heavy flavour production*, *JHEP* **08** (2003) 007 [hep-ph/0305252] [SPIRES].

[28] S. Frixione, P. Nason and G. Ridolfi, *A positive-weight next-to-leading-order monte carlo for heavy flavour hadroproduction*, *JHEP* **09** (2007) 126 [arXiv:0707.3088] [SPIRES].

[29] S. Frixione, E. Laenen, P. Motylinski and B.R. Webber, *Angular correlations of lepton pairs from vector boson and top quark decays in Monte Carlo simulations*, *JHEP* **04** (2007) 081 [hep-ph/0702198] [SPIRES].

[30] W.T. Giele, Z. Kunszt and K. Melnikov, *Full one-loop amplitudes from tree amplitudes*, *JHEP* **04** (2008) 049 [arXiv:0801.2237] [SPIRES].

[31] R.K. Ellis, W.T. Giele, Z. Kunszt and K. Melnikov, *Masses, fermions and generalized D-dimensional unitarity*, arXiv:0806.3467 [SPIRES].

[32] S. Dittmaier, P. Uwer and S. Weinzierl, *NLO QCD corrections to $t\bar{t}$ + jet production at hadron colliders*, *Phys. Rev. Lett.* **98** (2007) 262002 [hep-ph/0703120] [SPIRES].

[33] S. Dittmaier, P. Uwer and S. Weinzierl, *Hadronic top-quark pair production in association with a hard jet at next-to-leading order QCD: phenomenological studies for the Tevatron and the LHC*, *Eur. Phys. J.* **C 59** (2009) 625 [arXiv:0810.0452] [SPIRES].

[34] F.A. Berends and W.T. Giele, *Recursive calculations for processes with n gluons*, *Nucl. Phys.* **B 306** (1988) 759 [SPIRES].

[35] R.K. Ellis, W.T. Giele and Z. Kunszt, *A Numerical Unitarity Formalism for Evaluating One-Loop Amplitudes*, *JHEP* **03** (2008) 003 [arXiv:0708.2398] [SPIRES].

[36] G. Ossola, C.G. Papadopoulos and R. Pittau, *Reducing full one-loop amplitudes to scalar integrals at the integrand level*, *Nucl. Phys.* **B 763** (2007) 147 [hep-ph/0609007] [SPIRES].

[37] S. Catani and M.H. Seymour, *A general algorithm for calculating jet cross sections in NLO QCD*, *Nucl. Phys.* **B 485** (1997) 291 [*Erratum ibid.* **B 510** (1998) 503] [hep-ph/9605323] [SPIRES].

[38] S. Catani, S. Dittmaier, M.H. Seymour and Z. Trócsányi, *The dipole formalism for*

JHEP08(2009)049

next-to-leading order QCD calculations with massive partons, *Nucl. Phys.* **B 627** (2002) 189 [hep-ph/0201036] [SPIRES].

[39] M. Jezabek and J.H. Kuhn, *QCD Corrections to Semileptonic Decays of Heavy Quarks*, *Nucl. Phys.* **B 314** (1989) 1 [SPIRES];
A. Czarnecki, *QCD corrections to the decay $t \to Wb$ in dimensional regularization*, *Phys. Lett.* **B 252** (1990) 467 [SPIRES];
C.S. Li, R.J. Oakes and T.C. Yuan, *QCD corrections to $t \to W^+ b$*, *Phys. Rev.* **D 43** (1991) 3759 [SPIRES].

[40] J.M. Campbell, R.K. Ellis and F. Tramontano, *Single top production and decay at next-to-leading order*, *Phys. Rev.* **D 70** (2004) 094012 [hep-ph/0408158] [SPIRES].

[41] T. Stelzer and W.F. Long, *Automatic generation of tree level helicity amplitudes*, *Comput. Phys. Commun.* **81** (1994) 357 [hep-ph/9401258] [SPIRES].

[42] See R.K. Ellis and J. Campbell, *MCFM - Monte Carlo for FeMtobarn processes*, http://mcfm.fnal.gov/;
R.K. Ellis, *An update on the next-to-leading order Monte Carlo MCFM*, *Nucl. Phys. Proc. Suppl.* **160** (2006) 170 [SPIRES].

[43] J. Pumplin et al., *New generation of parton distributions with uncertainties from global QCD analysis*, *JHEP* **07** (2002) 012 [hep-ph/0201195] [SPIRES].

[44] P.M. Nadolsky et al., *Implications of CTEQ global analysis for collider observables*, *Phys. Rev.* **D 78** (2008) 013004 [arXiv:0802.0007] [SPIRES].

[45] S. Catani, Y.L. Dokshitzer and B.R. Webber, *The K^- perpendicular clustering algorithm for jets in deep inelastic scattering and hadron collisions*, *Phys. Lett.* **B 285** (1992) 291 [SPIRES].

[46] A. Banfi, G.P. Salam and G. Zanderighi, *Infrared safe definition of jet flavor*, *Eur. Phys. J.* **C 47** (2006) 113 [hep-ph/0601139] [SPIRES].

[47] A. Kharchilava, *Top mass determination in leptonic final states with J/ψ*, *Phys. Lett.* **B 476** (2000) 73 [hep-ph/9912320] [SPIRES].

[48] T. Arens and L.M. Sehgal, *Azimuthal correlation of charged leptons produced in $p\bar{p} \to t\bar{t}$ + ..*, *Phys. Lett.* **B 302** (1993) 501 [SPIRES].

[49] Z. Bern, L.J. Dixon and D.A. Kosower, *One loop corrections to two quark three gluon amplitudes*, *Nucl. Phys.* **B 437** (1995) 259 [hep-ph/9409393] [SPIRES].

[50] Z. Nagy and Z. Trócsányi, *Next-to-leading order calculation of four-jet observables in electron positron annihilation*, *Phys. Rev.* **D 59** (1999) 014020 [*Erratum ibid.* **D 62** (2000) 099902] [hep-ph/9806317] [SPIRES].

[51] Z. Nagy, *Next-to-leading order calculation of three jet observables in hadron hadron collision*, *Phys. Rev.* **D 68** (2003) 094002 [hep-ph/0307268] [SPIRES].

JHEP08(2009)049